Journal of Ceramic Processing Research. Vol. 13, No. 6, pp. 683~687 (2012)

J O U R N A L O F
Ceramic Processing Research

Comparison of fracture toughness evaluating methods in 3Y-TZP ceramics reinforced with Al_2O_3 particles

Jingwen Xu[a], Dongxu Tang[a], Ki-Ju Lee[a], Hyung-Bong Lim[a], K. Park[b] and Won-Seung Cho[a,*]
[a]*School of Materials Science and Engineering, Inha University, Incheon, Korea*
[b]*Nanotechnology and Advanced Materials Engineering, Sejong University, Seoul 143-741, Korea*

3Y-TZP/Al_2O_3 composites containing 0 to 30 vol% alumina were fabricated by sintering at 1550 °C for 2 h. The fracture toughness was measured using a range of techniques. The fracture toughness measured using the single edge V-notched beam (SEVNB) method, the controlled surface flaw and indentation strength in bending methods decreased with increasing Al_2O_3 content. This can be explained by the increased critical transformation stress, decreased volume fraction of transformable t-ZrO_2 and increased residual tensile stress. In contrast, the value obtained by the indentation fracture (IF) method showed an increasing tendency. Accordingly, the IF method is unsuitable for evaluating the fracture toughness of 3Y-TZP/Al_2O_3 composites. The SEVNB method is considered one of the most reliable methods for determining the fracture toughness of ceramic materials.

Key words: 3Y-TZP/Al_2O_3 composites, Fracture toughness, Single edge V-notched beam, Residual stress.

Introduction

Zirconia (ZrO_2) ceramics are used widely in dentistry owing to their excellent mechanical properties [1]. It is believed that a stress-induced, tetragonal zirconia to monoclinic zirconia phase transformation can increase the fracture toughness. This phase transformation is accompanied by a substantial increase in volume (~ 4 %), which can cause a compressive stress on a ground surface or in the vicinity of a crack tip. This clamping constraint on the crack tip needs to be overcome for an advancing crack to propagate [2]. 3 mol% Y_2O_3 stabilized ZrO_2 (3Y-TZP) ceramics have attracted particular attention due to the large range of solid solubility for yttria in tetragonal zirconia and the low eutectoid temperature (~ 550 °C), which avoids the decomposition of both tetragonal and cubic solid solutions during cooling from the sintering temperature [3].

The fracture toughness is an important mechanical property for the utilization of 3Y-TZP as dental ceramics. On the other hand, the toughness of 3Y-TZP ceramics can vary widely (from 4.25 to 10 $MPam^{1/2}$) depending on the fracture toughness evaluation methods used [4-8]. Moreover, confusing results concerning the effect of Al_2O_3 on the fracture toughness of Y-TZP ceramics have been reported. Santos *et al*. [9] reported that the addition of Al_2O_3 had no significant effect on the fracture toughness, whereas Choi and Bansal [10] stated that the fracture toughness increased with increasing Al_2O_3 content. Nevarez-Rascon *et al.* [11] found that 3Y-TZP containing 20 wt% Al_2O_3 exhibited the maximum fracture toughness of the samples examined. These discrepancies might be due to different microstructures, such as grain size, porosity, purity, Al_2O_3 particle size. Therefore, it is necessary to clarify the effect of an Al_2O_3 addition on the fracture toughness of ZrO_2/Al_2O_3 composites.

The single edge V-notched beam (SEVNB) method is considered one of the most reliable methods for evaluating the fracture toughness of ceramics. In the present study, alumina-reinforced zirconia composites, containing 0 to 30 vol% alumina, were fabricated by sintering. This study evaluated the fracture toughness of 3Y-TZP/Al_2O_3 ceramics using the SEVNB method, and compared the results with those obtained using different methods, such as indentation fracture (IF), indentation strength in bending (ISB) and controlled surface flaw (CSF) methods.

Experimental procedure

Preparation of materials

3 mol% Y_2O_3 stabilized ZrO_2 (> 99.7%, 90 nm, Tosoh, Japan) and Al_2O_3 (99.99%, 0.33 μm, Sumitomo, Japan) were used as the starting materials. Different amounts of Al_2O_3 ranging from 0 to 30 vol% were added to the ZrO_2 powders. The mixed powders were ball-milled for 24 h in an ethanol medium using a plastic jar and ZrO_2 balls. The mixed powders were dried on a hot plate and stirred to avoid gravity-induced segregation. After drying and sieving, the mixed powders were pressed uniaxially at 100 MPa, and cold isostatically

*Corresponding author:
Tel : +82-32-860-7528
Fax: +82-32-862-5546
E-mail: wscho@inha.ac.kr

pressed at 150 MPa. The green bodies obtained were sintered at 1550 °C for 2 h in air. After grinding (220 grit diamond wheel) and polishing (1 µm diamond paste), rectangular specimens with dimensions of $3 \times 4 \times 40$ mm were obtained. After polishing, some specimens were annealed at 1200 °C for 1 h in air to estimate the residual stress generated during polishing.

Measurement of fracture toughness

The SEVNB method was carried out using both as-polished and annealed specimens. The surface of the specimens (3×40 mm in size) were pre-notched using a diamond cutting wheel (thickness: approximately 250 µm). The depths of the notch were approximately 0.5 mm according to the ISO standard [12]. Fig. 1 shows the apparatus for forming a groove using a resin bonded diamond cutting wheel. The apparatus was designed specially to introduce sharp V-notches, as shown in Fig. 2(a). The notches were then sharpened with a razor blade by polishing the notch tip with diamond paste (1 µm) placed into the notch. The V-notch root radii were measured by scanning electron microscopy (SEM) of the notch tip of each specimen. Fig. 2(b) shows an example of a V-notch. The sharpened notch root radius of the specimen in the micrograph was approximately 17.5 µm. For a valid K_{IC} measurement, the notch root radii and depths of specimens were kept to less than 20 µm and 0.8 mm, respectively. The specimens with sharpened notches were finally loaded in a four-point bending test jig (outer span: 30 mm, inner span; 10 mm) under a cross head speed of 0.5 mmminute^{-1}. The equation is described as follows:

$$K_{IC}=\sigma\sqrt{a}Y=\frac{p}{b\sqrt{w}}\times\frac{S_1-S_2}{w}\times\frac{3\sqrt{\alpha}}{2(1-\alpha)^{1.5}}Y \qquad (1)$$

For four-point bending test, Y is calculated by the following equation:

$$Y=1.9887-1.326\alpha-\frac{(3.49-0.68\alpha+1.35\alpha^2)\alpha(1-\alpha)}{(1+\alpha)^2},\alpha=\frac{a}{w} \qquad (2)$$

where K_{IC} is the fracture toughness, σ is the fracture strength, P is the fracture load, b is the specimen thickness, w is the specimen width, S_1 and S_2 are support spans ($S_1 > S_2$), and Y is the stress intensity shape factor.

For comparison, the fracture toughness was also measured using indentation based methods, such as the IF [13], ISB [14] and CSF [15]. In the IF method, Vickers indentations were introduced to the mirror-like sample surface using a hardness tester (Akashi, Model AVK-C0) under a 98 N load with a dwell time of 15 s. The equation proposed by Evans [16] was used to calculate the fracture toughness.

For the ISB method, Vickers indentations were produced at the center of the specimen's mirror-like surface. The specimens were then fractured using a 3-point bending test. The crosshead speed was 0.5 mmminute^{-1}. The fracture stress (σ_f) was calculated using the following equation [17]:

$$\sigma_f=\frac{3WL}{2BD^2} \qquad (3)$$

where W is the breaking load, L is the span, B is the specimen's width and D is the specimen's thickness. The fracture toughness was calculated using the equation proposed by Chantikul *et al.* [14] as follows:

$$K_{IC}=0.59\left(\frac{E}{H}\right)^{\frac{1}{8}}\left(\sigma_f p^{\frac{1}{2}}\right)^{\frac{3}{4}} \qquad (4)$$

where E is the elastic modulus, H is the hardness and P is the indentation load.

For the CSF method, the specimens were precracked

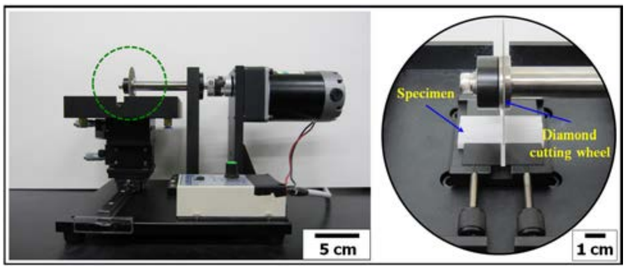

Fig. 1. Apparatus to form a groove using a resin bonded diamond cutting wheel (thickness: approximately 250 µm).

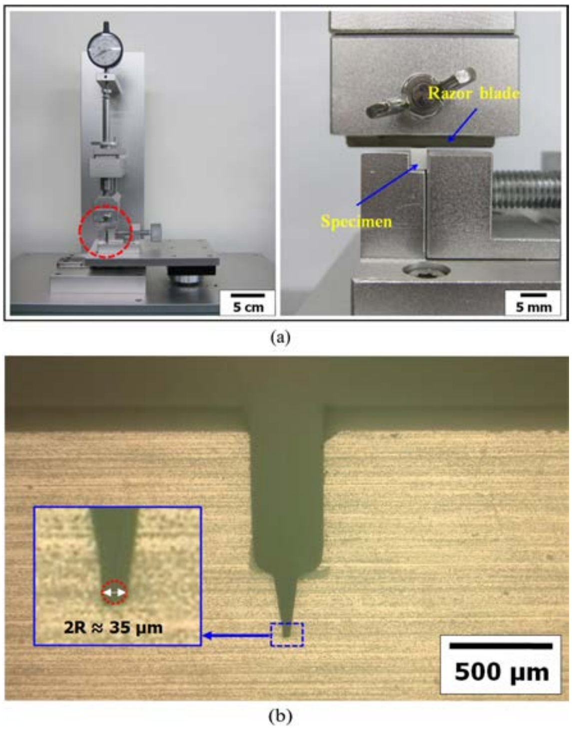

Fig. 2. Apparatus to introduce sharp V-notch using a razor blade (a) and an example of a sharpened V-notch in a Al_2O_3/3Y-TZP specimen (b).

by introducing a 98 N Vickers indentation at the center of the polished surface. The indented surface was then polished with diamond paste to remove a ~ 0.06 mm layer to eliminate the effect of residual stress on the fracture toughness caused by the indentation [18]. The specimens were tested using a 4-point bending method. The fracture toughness was calculated using the equations reported by Govila as follows [19]:

$$K_I = \sigma M(\pi a/Q)^{1/2} \qquad (5)$$

where σ is the fracture stress, a is the flaw depth, and M and Q are numerical factors related to the flaw and specimen geometry, respectively. For semicircular flaws, M = 1.03. Q was obtained using the following equation:

$$Q = \Phi^2 - 0.212(\sigma/\sigma_{ys})^2 \qquad (6)$$

$$Q \approx \Phi^2$$

where σ_{ys} is the yield stress, $0.212(\sigma/\sigma_{ys})^2$ is a plastic-zone correction factor (this factor is negligible for brittle failure in ceramics), and Φ is an elliptic integral of the second kind:

$$\Phi = \int_0^{\pi/2} [sin^2\theta + (a/c)^2 cos^2\theta]^{1/2} d\theta \qquad (7)$$

where 2a is the depth of a semielliptical crack and 2c is the total crack length at the free surface.

Results and discussion

Fig. 3 presents the fracture toughness of the as-polished and annealed specimens as a function of the Al_2O_3 content using the SEVNB method. The fracture toughness decreased with increasing Al_2O_3 content. The fracture toughness of the polished specimens was higher than those of the annealed specimens due to the residual compressive stresses introduced during polishing.

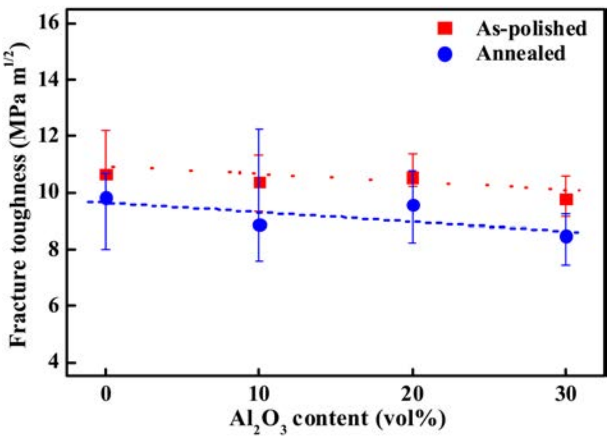

Fig. 3. Fracture toughness (SEVNB method) of the 3Y-TZP/Al_2O_3 composites.

This decreasing tendency could be attributed to the increased critical transformation stress (σ_c), the decreased volume fraction of transformable t-ZrO_2 and the increased residual tensile stress [20].

Table 1 lists the critical transformation stress, fracture toughness increment (ΔK), transformed zone depth (h) and volume fraction (V_m) of the monoclinic phase. The critical transformation stress increased with increasing Al_2O_3 content, suggesting that extra stress should be applied to induce a t → m transformation with increasing Al_2O_3 content, which resulted in a decreased transformation zone and fracture toughness. The depth of the transformed zone decreased with increasing Al_2O_3 content, suggesting that less t → m transformation occurred with increasing Al_2O_3 addition: The decreasing t → m transformation would result in a decrease in fracture toughness [20].

The thermal residual stresses developed in the composite ceramics play an important role in the fracture toughness of composites. Thermal residual stresses can be introduced due to thermal expansion mismatch between ZrO_2 (10.3×10^{-6}/°C) and Al_2O_3 (8.1×10^{-6}/°C) [21]. A radial compressive stress and hoop tensile stress were developed in the 3Y-TZP/Al_2O_3 composite. The hoop tensile stress increased with increasing Al_2O_3 content. Crack deflection could not be expected under such a tensile residual stress circumstance. Therefore, a residual tensile stress may be another reason for the decreased fracture toughness [20].

For the CSF method, the fracture surfaces were examined by SEM to observe the semi-elliptical median cracks of the composites, as shown in Fig. 4. The lengths (2a and 2c in Eq. 5) of the semi-elliptical surface cracks in the 3Y-TZP/Al_2O_3 composites were measured to calculate the fracture toughness.

Fig. 5 shows the fracture toughness as a function of the Al_2O_3 content tested using the CSF and ISB methods. The fracture toughness measured using the CSF and ISB methods showed a decreased tendency with increasing Al_2O_3 content, even though the decreasing fracture toughness was not as pronounced as observed in the ISB method.

Table 1. Critical transformation stress (σ_c), fracture toughness increment (ΔK), transformed zone depth (h) and volume fraction of each composite.

Samples	Measured at fracture surface		ΔK (MPam$^{1/2}$)	σ_c (GPa)
	V_m (%)	h (μm)		
3Y-TZP	22.11	3.89	1.21	1.271
3Y-TZP/10A	20.97	3.66	1.16	1.051
3Y-TZP/20A	12.86	2.12	0.57	1.437
3Y-TZP/30A	8.04	1.28	0.29	1.451

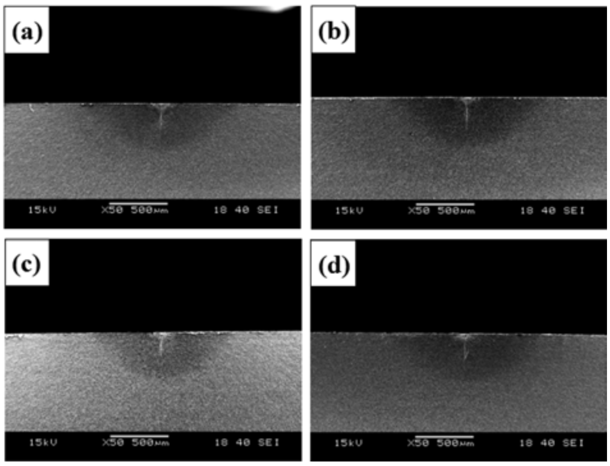

Fig. 4. Semi-elliptical surface cracks in the 3Y-TZP/Al_2O_3 composites; (a) 3Y-TZP, (b) 3Y-TZP/10A, (c) 3Y-TZP/20A and (d) 3Y-TZP/30A.

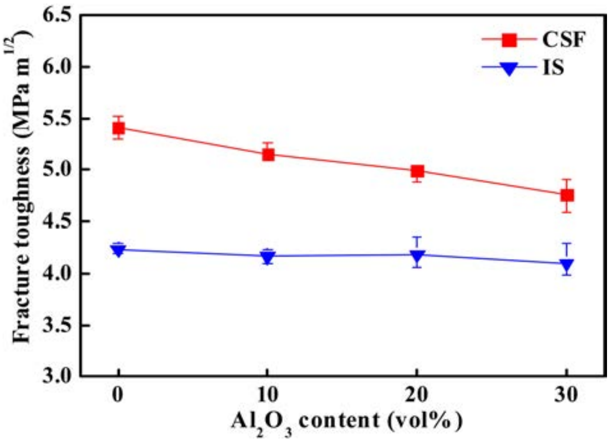

Fig. 5. Fracture toughness (CSF and IS methods) of the 3Y-TZP/Al_2O_3 composites.

Fig. 6 presents the fracture toughness of 3Y-TZP/Al_2O_3 measured using the IF method. The test was carried out at 98 N. In general, ceramics are finished by conventional grinding followed by diamond polishing or lapping. Conventional polishing employs high loads and diamond abrasives, which can cause a residual stress on the surface of the ceramics. The effect of residual stress on the fracture toughness obtained by the IF method was assessed by testing both polished and annealed specimens as well as ground and polished specimens. The fracture toughness of the polished and annealed specimens increased slightly with increasing Al_2O_3 content, whereas the fracture toughness of the ground and polished specimens appears to be sensitive to Al_2O_3 addition. The value increased dramatically when the Al_2O_3 content was 10 vol% and reached saturation at 6.9 MPam$^{1/2}$. The specimens without heat treatment showed higher fracture toughnesses that the annealed ones. To explain the increase in fracture toughness, the residual compressive stress generated during grinding and polishing were estimated using the following equation [22]:

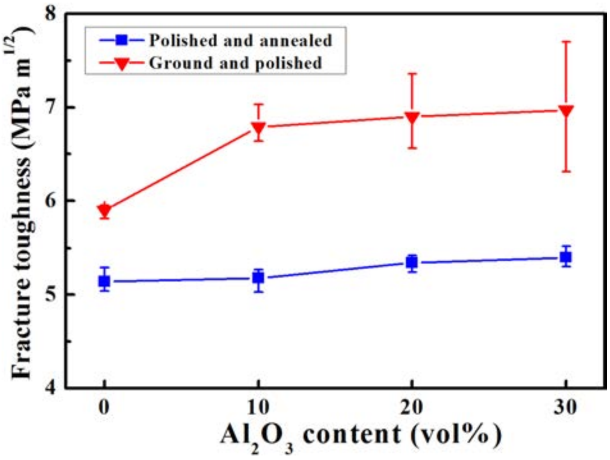

Fig. 6. Fracture toughness (IF method) of the 3Y-TZP/Al_2O_3 composites.

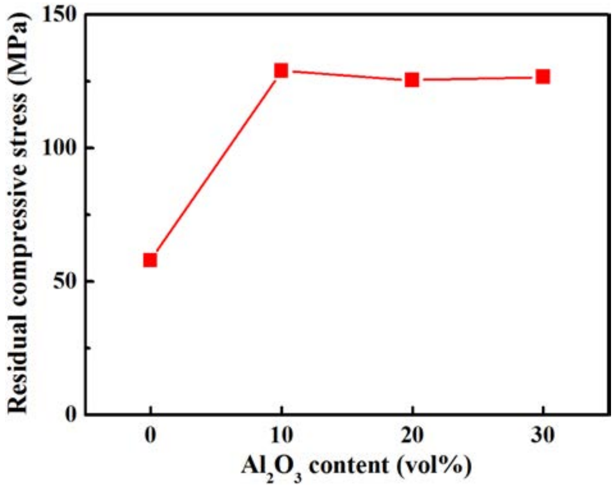

Fig. 7. Estimated residual compressive stress generated during the grinding and polishing procedures in the 3Y-TZP/Al_2O_3 composites.

$$\sigma_r = \frac{K_p - K_a}{2(c/\pi)^{1/2}} \tag{8}$$

where σ_r is the residual stress (MPa), K_p is the fracture toughness (IF) of the ground and polished sample, K_a is the fracture toughness (IF) of the annealed sample and c is the crack length (μm). Fig. 7 shows the estimated residual compressive stresses generated during the grinding and polishing procedures in the 3Y-TZP/Al_2O_3 composites. The residual stress was also sensitive to the addition of Al_2O_3 and presented a dramatic jump at 10 vol%. This result is consistent with the fracture toughness of the polished and annealed specimens. The results also suggest that the residual stress generated during polishing has a significant effect on the measured fracture toughness.

The effects of the indentation load on the fracture toughness (IF method) in the 3Y-TZP/Al_2O_3 composites were also investigated (Fig. 8). The fracture toughnesses were measured using ground and polished specimens. For all the composites, the fracture toughness decreased with increasing load. The 3Y-TZP/Al_2O_3 composites

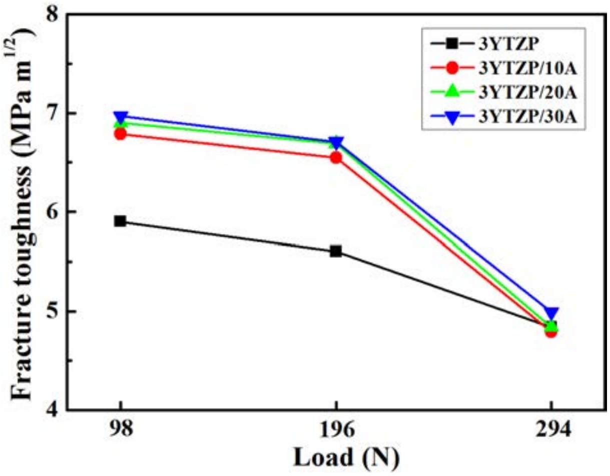

Fig. 8. Effect of the indentation load on the fracture toughness (IF method) in the 3Y-TZP/Al_2O_3 composites. The toughnesses of the ground and polished specimens were measured.

showed higher values than the 3Y-TZP ceramics until 196 N. However, there was no appreciable difference in fracture toughness at 294 N between 3Y-TZP/Al_2O_3 composites and 3Y-TZP ceramics. Based on this study, the IF method is unsuitable for evaluating the fracture toughness of 3Y-TZP/Al_2O_3 composites. Overall, the SEVNB method is believed to be the most reliable method for determining the fracture toughness of ceramic materials.

Conclusions

3Y-TZP/Al_2O_3 composites containing 0 to 30 vol% of Al_2O_3 were fabricated by pressureless sintering, and the fracture toughness was evaluated using a range of methods. The fracture toughness measured by the SEVNB method decreased with increasing Al_2O_3 content, which was explained by the increasing critical transformation stress, decreasing volume fraction of transformable t-ZrO_2 and increasing residual tensile stress. The fracture toughness tested using the CSF and ISB methods showed a similar tendency to that observed using the SEVNB method. The IF method was found to be unsuitable for measuring the fracture toughness of 3Y-TZP/Al_2O_3 composites. Overall, the SEVNB method is considered the most reliable method for determining the fracture toughness of 3Y-TZP/ Al_2O_3 ceramic composites.

Acknowledgement

This study was supported by Basic Science Research Program through a grant from the National Research Foundation of Korea (NRF) funded by the Ministry of Education, Science and Technology (2009-0077518).

References

1. I. Denry and J.R. Kelly, Dent. Mater., 24 (2008) 299-307.
2. J. Wang and R. Stevens, J. Mater. Sci., 24 (1989) 3421-3440.
3. I. Nettleship and R. Stevens, Int. J. High. Technol. Ceram., 3 (1987) 1-32.
4. B.A. Cottom and M.J. Mayo, Scr. Mater., 34 (1996) 809-814.
5. O. Vasylkiv, Y. Sakka and V. Skorokhod, J. Am. Ceram. Soc., 86 (2003) 299-304.
6. J. Eichler, J. Rödel, U. Eisele and M. Hoffman, J. Am. Ceram. Soc., 90 (2007) 2830-2836.
7. M. Trunec and Z. Chlup, Scripta Mater., 61 (2009) 56-59.
8. C. Piconi and G. Maccauro, Biomaterials, 20 (1999) 1-25.
9. C. Santos, L. Teixeira, J. Daguano, S. Rogero, K. Strecker and C. Elias, Ceram. Int., 35 (2009) 709-718.
10. S. Choi and N. Bansal, Ceram. Int., 31 (2005) 39-46.
11. A. Nevarez-Rascon, A. Aguilar-Elguezabal, E. Orrantia and M. Bocanegra-Bernal, Int. J. Refract. Met. Hard Mater., 27 (2009) 962-970.
12. ISO 6872, Fracture toughness: single edge V-notched beam method, (2008) (E).
13. K. Niihara, Ceram., 20 (1985) 12-18.
14. P. Chantikul, G.R. Anstis, B.R. Lawn and D.B. Marshall, J. Am. Ceram. Soc., 64 (1981) 539-544.
15. J.J. Petrovic and M.G. Mendiratta, in: S. Freiman (Eds.), Fracture Mechanics Applied to Brittle Materials, ASTM, West Conshohocken, PA, (1979) 83-102.
16. A.G. Evans, in: S. Freiman (Eds.), Fracture Mechanics Applied to Brittle Materials, ASTM, Philadelphia, PA, (1979) 112-135.
17. ISO 6872, Calculation of strength: Three-point flexture, (2008) (E).
18. J.F. Li and R. Watanabe, J. Am. Ceram. Soc., 78 (1995) 1079-1082.
19. R.K. Govila, J. Am. Ceram. Soc., 63 (1980) 319-326.
20. D. Tang, K.J. Lee, J. Xu, H.B. Lim, C.H. Lee and W.S. Cho, Met. Mater. Int., in press (2011).
21. K.K. Chawla, Ceramic matrix composite, Kluwer Academic Publishers, Norwell, (2003) 263-291.
22. H. Wu, S.G. Roberts and B. Derby, Acta. Mater., 49 (2001) 507-517.